

The stability and mixed conductivity in La and Fe doped SrTiO₃ in the search for potential SOFC anode materials

D.P. Fagg^{a,*}, V.V. Kharton^{a,b}, A.V. Kovalevsky^b, A.P. Viskup^b,
E.N. Naumovich^b, J.R. Frade^a

^a*Ceramics and Glass Engineering Department (UIMC), University of Aveiro, 3810 Aveiro, Portugal*

^b*Institute of Physicochemical Problems, Belarus State University, 220080 Minsk, Republic of Belarus*

Received 4 September 2000; received in revised form 7 November 2000; accepted 15 November 2000

Abstract

Both physical properties and the level of mixed conduction obtained in La and Fe doped SrTiO₃ are widely influenced by composition. In contrast to La free compositions, La containing compositions show high stability against reaction with yttria stabilised zirconia (YSZ) and a closely matching thermal expansion coefficient ($\sim 1 \times 10^{-5} \text{ K}^{-1}$). Faradaic efficiency measurements for Sr_{0.97}Ti_{0.6}Fe_{0.4}O_{3- δ} and La_{0.4}Sr_{0.5}Ti_{0.6}Fe_{0.4}O_{3- δ} show ionic transference numbers in air between 5×10^{-3} to 4×10^{-2} , and 2×10^{-4} to 6×10^{-4} respectively, decreasing with decreasing temperature. The substitution of La for Sr is observed to deplete the level of both ionic and total conductivity obtained in air. © 2001 Published by Elsevier Science Ltd.

Keywords: Electrical conductivity; Ionic conductivity; Perovskites; Strontium titanate ferrites; Thermal expansion

1. Introduction

The co-existence of high electronic conductivity and relatively good oxygen ion conductivity has been suggested to enhance the performance of electrode materials for solid oxide fuel cells (SOFCs) due to the extension of the electrochemical reaction over the entire electrode surface rather than localised at triple contact areas.^{1,2} This type of approach has failed, however, in what concerns the anodic reaction because well known oxide materials with high electronic conductivity and relatively good ionic conductivity usually undergo degradation on attaining moderately reducing conditions and cannot be used in very reducing conditions. For example La_{1- x} Sr _{x} CoO_{3- δ} materials possess high p -type electronic conductivity and relatively good ionic conductivity but the stability range reduces to $p\text{O}_2 > 10^{-7} \text{ atm}$ at 1000°C.³ The main electronic contribution of mixed conducting materials, having a sufficient stability domain with respect to oxygen chemical potential

variation, typically changes from p -type in oxidising conditions to n -type in reducing conditions. The n -type behaviour is thus often typical of atmosphere containing significant fractions of a fuel (H₂, CH₄, etc.). Unfortunately, the highest values of n -type conductivity attained by known ceramic materials remains orders of magnitude lower than the values of conductivity attained by p -type conductors such as La_{1- x} Sr _{x} CoO_{3- δ} . In addition, attempts to enhance the n -type contribution usually deplete the ionic conductivity, as found for typical electrolyte materials, thus raising doubts about the possibility of obtaining sufficiently good mixed conducting electrodes for reducing conditions.

Nevertheless, the dependence of conductivity of SrTi_{1- x} Fe _{x} O_{3- δ} on the oxygen partial pressure indicated that the ionic conductivity might attain values of about 0.2 S/cm at 1000°C, with major electronic contributions in oxidizing conditions (p -type), or for sufficiently reducing conditions (n -type).⁴ The good mixed conductivity of these materials was also confirmed by electrochemical permeability measurements.⁵ This work offers preliminary studies in air of the stability of two of the more promising compositions Sr_{0.9}Ti_{0.6}Fe_{0.4}O_{3- δ} , Sr_{0.97}Ti_{0.6}Fe_{0.4}O_{3- δ} and also the La doped material La_{0.4}Sr_{0.5}Ti_{0.6}Fe_{0.4}O_{3- δ} with respect to reactions with 8% yttria

* Corresponding author. Tel.: +351-3810-092.

E-mail address: duncan@cv.ua.pt (D.P. Fagg).

stabilised zirconia (YSZ) the most common SOFC electrolyte, thermal expansion behaviour and the influence of La doping on conductivity.

2. Experimental methods

Powders of $\text{Sr}_{0.9}\text{Ti}_{0.6}\text{Fe}_{0.4}\text{O}_{3-\delta}$, $\text{Sr}_{0.97}\text{Ti}_{0.6}\text{Fe}_{0.4}\text{O}_{3-\delta}$ (STFO) and $\text{La}_{0.4}\text{Sr}_{0.5}\text{Ti}_{0.6}\text{Fe}_{0.4}\text{O}_{3-\delta}$ (LSTFO) were prepared by solid state reaction from dried TiO_2 , Fe_2O_3 , La_2O_3 and SrCO_3 . Calcination of STFO at 1100°C and LSTFO at 1300°C , for 12 h, was followed by milling to destroy agglomerates, and subsequent preparation of dense pellets by uniaxial pressing and sintering for 5 h at 1400°C and 1600°C , respectively. The use of a higher temperature in the LSTFO case was found to be obligatory in order to achieve phase purity and good density. A-site deficiency was introduced in both compositions to improve the long term stability of these materials, relative to those with unit A/(Ti + Fe) ratio.⁶

X-ray diffraction results using a Rigaku Geigerflex diffractometer indicated all samples were monophasic. STFO compositions exhibit the cubic perovskite structure (space group Pm3m) whilst the La containing LSTFO composition exhibit an orthorhombic perovskite structure (Pnma). Fixed frequency (10 kHz) ac conductivity measurements were made as a function of the oxygen partial pressure (from air to about 10^{-15} Pa), in a controlled atmosphere furnace. Details on the experimental set-up and corresponding performance are presented and discussed elsewhere.⁷ Impedance spectra were obtained by a 4-electrode ac method using a frequency response analyser HP428A. The level of ionic conductivity was separated from the total conductivity by the use of the Faradaic efficiency technique. This

technique is explained in detail elsewhere.⁸ The reactivity between 8 mol% YSZ and STFO was assessed by firing intimate powder mixtures of these materials, (1:1 ratio of YSZ to STFO or LSTFO by weight), and firing for 12 h in air, at different temperatures (Fig. 1). Thermal expansion data is measured by a quartz dilatometer DKV-5A in air between 25 – 850°C .

3. Results and discussion.

X-ray powder diffractograms of the intimate powder mixtures (Fig. 1), show that in the STFO compositions the YSZ peaks remain nearly unchanged after sintering at 1250°C , whilst the cubic perovskite phase undergoes significant structural changes. The intensities of the original perovskite peaks (e.g. at $2\theta = 32.3$, 46.5 and 57.8) decrease, whilst new peaks (e.g. at $2\theta = 31.7$, 45.7 and 56.7) indicate the presence a new phase. It has been suggested⁶ that an increase in A-site deficiency would lead to a reduction in the chemical reactivity of these types of compositions. If one compares the relative intensities of the YSZ peaks and those of the reaction products formed, it is observed that the amount of reaction product formed in the case of $\text{Sr}_{0.9}\text{Ti}_{0.6}\text{Fe}_{0.4}\text{O}_{3-\delta}$ (Fig. 1b) is notably less for that for $\text{Sr}_{0.97}\text{Ti}_{0.6}\text{Fe}_{0.4}\text{O}_{3-\delta}$ (Fig. 1a) under the same reaction conditions. An increase in A-site vacancy concentration therefore leads to a reduction in the chemical reactivity between YSZ and STFO. The substitution of La for Sr on the A-site leads to further stabilisation of the perovskite material. No reaction products can be seen for an intimate mixture of $\text{La}_{0.4}\text{Sr}_{0.5}\text{Ti}_{0.6}\text{Fe}_{0.4}\text{O}_{3-\delta}$ and YSZ fired at the same conditions, the two phases remain distinct (Fig. 1c).

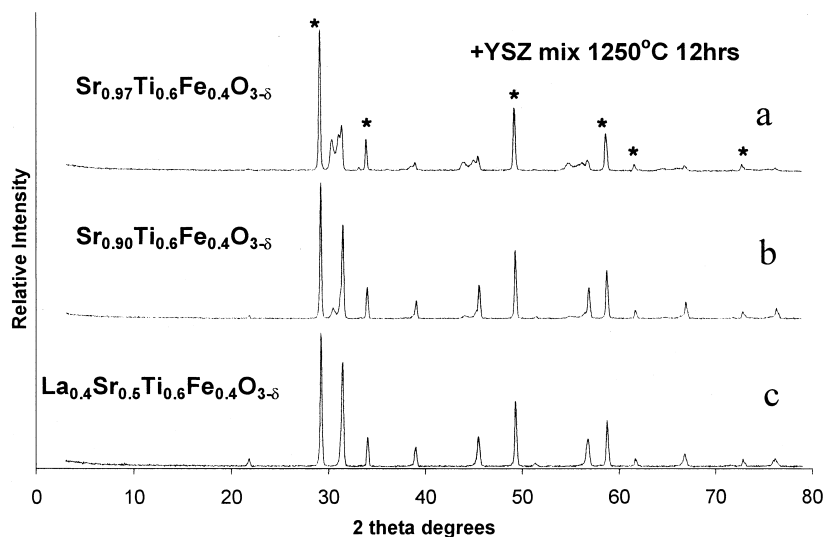


Fig. 1. Powder X-ray diffractograms showing the reactivity between intimate powder mixtures of 8 mol% yttria stabilised zirconia (YSZ) and STFO or LSTFO compositions fired at 1250°C for 12 h. Asterisks denote the positions of the YSZ reflections.

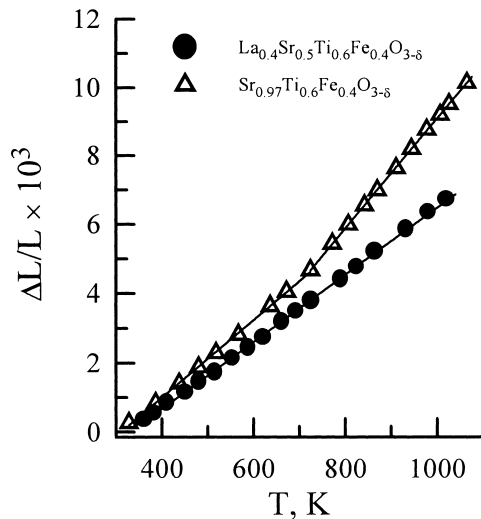


Fig. 2. Dilatometric curves of $\text{Sr}_{0.97}\text{Ti}_{0.6}\text{Fe}_{0.4}\text{O}_{3-\delta}$ and $\text{La}_{0.4}\text{Sr}_{0.5}\text{Ti}_{0.6}\text{Fe}_{0.4}\text{O}_{3-\delta}$ in air. Solid lines correspond to a best fit using linear regression model.

Fig. 2 compares the thermal expansion in air for the STFO and LSTFO compositions. The STFO composition shows a discontinuity in thermal expansion behaviour at approximately 720 K. This behaviour is suggested to be due to loss of oxygen at higher temperatures.⁹ Such a variation of thermal expansion coefficient with temperature is not exhibited by the LSTFO composition. Corresponding thermal expansion coefficients are summarised in Table 1. The SFTO composition offers a thermal expansion coefficient significantly greater than that of YSZ ($10 \times 10^{-6} \text{ K}^{-1}$) at elevated temperatures, whilst the LSTFO composition shows a good match with that of YSZ throughout the temperature range. This maybe an attractive property for the use of LSTFO in SOFCs.

The temperature dependence of the total conductivity in air for all compositions is shown in Fig. 3. It has been shown previously that SFTO compositions fired in air, contain large quantities of Fe^{4+} and that this concentration decreases with increasing temperature as more oxygen ion vacancies are formed.⁹ The break in the conductivity behaviour in the high temperature range suggests a semiconducting to metallic transition as found in other ceramic materials with high conductivity such as $\text{La}_{1-x}\text{Sr}_x\text{CoO}_3$.¹⁰

Table 1
Thermal expansion coefficients of perovskite oxide ceramics

Composition	T, K	Average TECs $\alpha \times 10^{-6}, \text{K}^{-1}$
$\text{La}_{0.4}\text{Sr}_{0.5}\text{Ti}_{0.6}\text{Fe}_{0.4}\text{O}_{3-\delta}$	300–1050	10.2 ± 0.1
$\text{Sr}_{0.97}\text{Ti}_{0.6}\text{Fe}_{0.4}\text{O}_{3-\delta}$	300–720	11.7 ± 0.2
	720–1070	16.60 ± 0.07

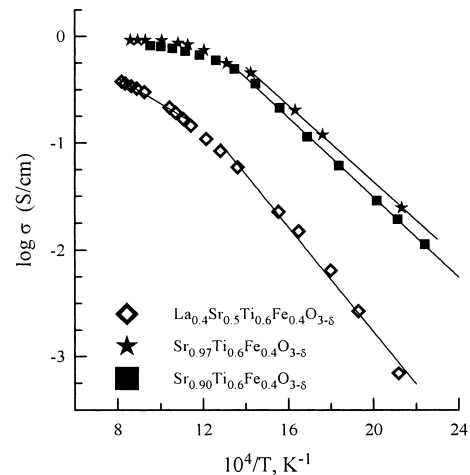


Fig. 3. Temperature dependence of the total electrical conductivity in air of $\text{Sr}_{0.97}\text{Ti}_{0.6}\text{Fe}_{0.4}\text{O}_{3-\delta}$, $\text{Sr}_{0.90}\text{Ti}_{0.6}\text{Fe}_{0.4}\text{O}_{3-\delta}$ and $\text{La}_{0.4}\text{Sr}_{0.5}\text{Ti}_{0.6}\text{Fe}_{0.4}\text{O}_{3-\delta}$. The solid lines correspond to the Arrhenius model.

The effect of La substitution can be charge compensated by a reduction in either the oxygen vacancy concentration or the concentration of Fe^{4+} present. The electroneutrality equation in this case can be written as:

$$[\text{La}_{\text{Sr}}^{\bullet}] + 2[\text{V}_{\text{O}}] + p = 2[\text{V}_{\text{Sr}}''] + [\text{Fe}_{\text{Ti}}'] + n$$

The lower conductivity of LSTFO observed in Fig. 3, can therefore be explained to be due to a lower electron hole concentration in this composition in oxidizing conditions.

The larger A-site vacancy concentration in $\text{Sr}_{0.9}\text{Ti}_{0.6}\text{Fe}_{0.4}\text{O}_{3-\delta}$ than in $\text{Sr}_{0.97}\text{Ti}_{0.6}\text{Fe}_{0.4}\text{O}_{3-\delta}$ can be accommodated by an increase in the oxygen vacancy concentration. As electron transfer in perovskites occurs via B–O–B bonds, an increase in oxygen vacancy concentration leads to decreasing mobility of electronic charge carriers and a decrease in conductivity. Another hypothesis is that the large cation vacancy concentration in this composition is accommodated by local ordering, forming microdomains of common related superstructure phases, for example brownmillerite,¹¹ and/or by strong local distortions of the crystal lattice, forming tungsten bronze-like domains.¹² In the case of brownmillerite-like microdomains, Fe ions are located in stable tetrahedral sites where their contribution to conduction is lower. Formation of distorted tungsten bronze-like domains would lead to deviating B–O–B angles from their ideal value, 180° , and thus to decreasing electron charge carrier mobility. As a result, the total conductivity of $\text{Sr}_{0.97}\text{Ti}_{0.6}\text{Fe}_{0.4}\text{O}_{3-\delta}$ in oxidizing conditions, predominantly electronic, is slightly higher than that of $\text{Sr}_{0.9}\text{Ti}_{0.6}\text{Fe}_{0.4}\text{O}_{3-\delta}$.

Fig. 4 shows the temperature dependence of the ionic conductivity in air. These values are calculated using the values of total conductivity shown in Fig. 3 and the

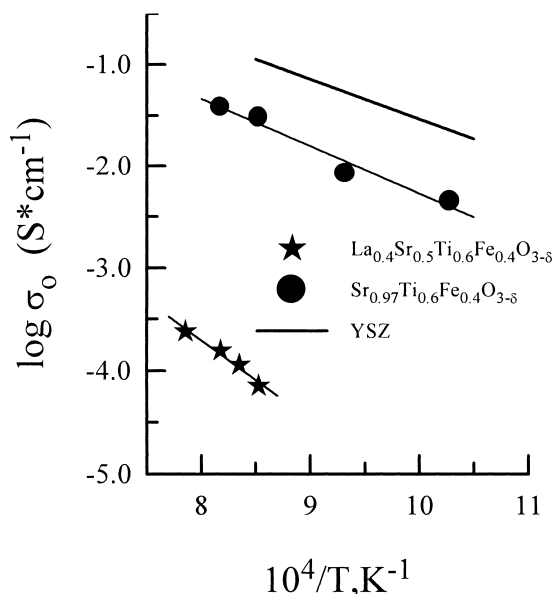


Fig. 4. Temperature dependence of the ionic conductivity of $Sr_{0.97}Ti_{0.6}Fe_{0.4}O_{3-\delta}$ and $La_{0.4}Sr_{0.5}Ti_{0.6}Fe_{0.4}O_{3-\delta}$ calculated from the values of total conductivity and oxygen ion transference numbers, determined by the Faradaic efficiency measurements under zero oxygen chemical potential gradient.

Table 2
Oxygen ion transference numbers, determined by the Faradaic efficiency measurements in air

Composition	T, K	t_0
$La_{0.4}Sr_{0.5}Ti_{0.6}Fe_{0.4}O_{3-\delta}$	1273	6.0×10^{-4}
	1223	4.2×10^{-4}
	1198	3.1×10^{-4}
	1173	2.1×10^{-4}
$Sr_{0.97}Ti_{0.6}Fe_{0.4}O_{3-\delta}$	1223	4.1×10^{-2}
	1173	3.3×10^{-2}
	1073	9.0×10^{-3}
	973	5.0×10^{-3}

Table 3
Regression parameters of the Arrhenius temperature dependencies of the *p*-type electronic and ionic conductivities in air

Conductivity	Composition	T, K	E_a , kJ/mol	$\ln A_0$ (S/cm)
Electronic	$La_{0.4}Sr_{0.5}Ti_{0.6}Fe_{0.4}O_{3-\delta}$	470–870	50 ± 2	11.9 ± 0.3
		870–1220	32.4 ± 0.8	9.35 ± 0.09
	$Sr_{0.97}Ti_{0.6}Fe_{0.4}O_{3-\delta}$	470–890	35 ± 3	11.5 ± 0.6
		890–1120	11 ± 1	8.2 ± 0.1
	$Sr_{0.90}Ti_{0.6}Fe_{0.4}O_{3-\delta}$	440–800	39.7 ± 0.6	12.3 ± 0.1
		840–1060	15.3 ± 0.7	8.54 ± 0.08
Ionic ^a	$La_{0.4}Sr_{0.5}Ti_{0.6}Fe_{0.4}O_{3-\delta}$	890–1120	158 ± 17	14 ± 2
	$Sr_{0.97}Ti_{0.6}Fe_{0.4}O_{3-\delta}$	970–1220	98 ± 12	13 ± 1

^a Ionic conductivity was calculated from the values of total conductivity and oxygen ion transference numbers, determined by the Faradaic efficiency measurements under zero oxygen chemical potential gradient.

values of ionic transport number (t_0) shown in Table 2 obtained by Faradaic efficiency measurements under zero oxygen chemical potential. LSTFO is shown to have a much lower ionic conductivity than STFO by over three orders of magnitude. Regression parameters of the Arrhenius temperature dependencies of the *p*-type electronic and ionic conductivities in air are shown in Table 3 using the standard Arrhenius model where A_0 is the pre-exponential factor and E_a is the activation energy for conduction.

$$\sigma = \frac{A_0}{T} \cdot \exp\left(-\frac{E_a}{RT}\right)$$

The principal factor affecting the level of ionic conduction is the higher activation energy for conduction in the LSTFO composition, suggesting a significant contribution for the formation of mobile vacancies in the case of LSTFO. An increase in temperature may increase the concentration of vacancies present due to oxygen exchange with the atmosphere and disorders the oxygen sublattice. The relative significance of these additional, thermally formed, vacancies to the overall level of ionic conductivity is probably much greater when one considers the LSTFO case, due to the lower intrinsic vacancy concentration in this composition than that of STFO. One must also consider the fact that the LSTFO composition exhibits an orthorhombic perovskite structure whilst the STFO composition exhibits a cubic perovskite structure. These two symmetries may not exhibit the same enthalpies for ion migration and vacancy formation. However, a change between these two symmetry types cannot expressly dictate that the LSTFO should exhibit such a large activation energy for conduction. Examples against this hypothesis are compositions such as $La_{0.9}Sr_{0.1}Ga_{0.8}Mg_{0.2}O_{3-\delta}$,¹³ which have the orthorhombic perovskite structure (Pnma) but which still exhibit very high levels of ionic conductivity with activation energies for conduction around 100 kJ mol⁻¹.

4. Conclusion

The substitution of La for Sr is observed to deplete the level of both ionic and total conductivity obtained in air. Faradaic efficiency measurements for $\text{Sr}_{0.97}\text{Ti}_{0.6}\text{Fe}_{0.4}\text{O}_{3-\delta}$ and $\text{La}_{0.4}\text{Sr}_{0.5}\text{Ti}_{0.6}\text{Fe}_{0.4}\text{O}_{3-\delta}$ show ionic transference numbers in air between 5×10^{-3} to 4×10^{-2} , and 2×10^{-4} to 6×10^{-4} , respectively, decreasing with decreasing temperature. La containing compositions show high stability against reaction with YSZ and a closely matching thermal expansion coefficient ($\sim 1 \times 10^{-5} \text{ K}^{-1}$).

References

1. Takeda, Y., Kanno, R., Noda, M., Tomida, Y. and Yamamoto, O., Phenomena of perovskite oxide electrodes with stabilised zirconia. *J. Electrochem. Soc.*, 1987, **134**, 2656–2661.
2. Gharbage, B., Pagnier, T. and Hammou, A., Oxygen reduction at $\text{La}_{0.5}\text{Sr}_{0.5}\text{MnO}_3$ thin film/yttria stabilised zirconia interface studied by impedance spectroscopy. *J. Electrochem. Soc.*, 1994, **141**, 2118–2121.
3. Nakamura, T., Petzow, G. and Gauckler, L. J., Stability of the perovskite phase LaBO_3 (B = V, Cr, Mn, Fe, Co, Ni) in reducing atmosphere, I. Experimental Results. *Mater. Res. Bull.*, 1979, **14**, 649–659.
4. Steinsvik, S., Bugge, R., Gjønnes, J., Taftø, J. and Norby, T., The defect structure of $\text{SrTi}_{1-x}\text{Fe}_x\text{O}_{3-y}$ ($x = 0-0.8$) investigated by electrical conductivity measurements and electron energy loss spectroscopy (EELS). *J. Phys. Chem. Solids*, 1997, **6**, 969–976.
5. Jurado, J. R., Figueiredo, F. M., Gharbage, B. and Frade, J. R., Electrochemical permeability of $\text{Sr}_{0.97}(\text{Ti,Fe})\text{O}_{3-\delta}$ materials. *Solid State Ionics*, 1999, **118**, 89–97.
6. Traqueia, L. S. M., Jurado, J. R. and Frade, J. R., In *Electroceramics V, Aveiro Portugal*, ed. J.L. Baptista, J.L. Labrincha and P.M. Vilarinho. 1996, **2**, pp. 151.
7. Marques, F. M. and Wirtz, B. G. P., Electrical properties of ceria-doped yttria. *J. Am. Ceram. Soc.*, 1991, **74**, 598–605.
8. Kharton, V. V., Kovalevsky, A. V., Viskup, A. P., Figueiredo, F. M., Frade, J. R., Yaremchenko, A. A. and Naumovich, E. N., Faradaic efficiency of $\text{Sr}_{0.97}\text{Ti}_{0.6}\text{Fe}_{0.4}\text{O}_{3-\delta}$ perovskite. *Solid State Ionics*, 2000, **128**, 117–130.
9. Ferreira, A. A., Abrantes, J. C. C., Jurado, J. R. and Frade, J. R., Oxygen stoichiometry of $\text{Sr}_{1-x}(\text{TiFe})\text{O}_{3-\delta}$ materials. *Solid State Ionics*, 2000, **135**, 761–764.
10. Kharton, V. V., Naumovich, E. N., Vecher, A. A. M. and Nikolaev, A. V., Oxide ion conduction in solid solutions $\text{Ln}_{1-x}\text{Sr}_x\text{CoO}_{3-\delta}$ (Ln = La, Pr, Nd). *J. Solid State Chem.*, 1995, **120**, 128–136.
11. Grenier, J.-C., Ea, N., Pouchard, M. and Hagenmüller, P., Structural transitions at high temperature in $\text{Sr}_2\text{Fe}_2\text{O}_5$. *J. Solid State Chem.*, 1985, **58**, 243–252.
12. Slater, P. R. and Irvine, J. T. S., Niobium based tetragonal tungsten bronzes as potential anodes for solid oxide fuel cells: synthesis and electrical characterisation. *Solid State Ionics*, 1999, **120**, 125–134.
13. Drennan, J., Zelizko, V., Hay, D., Ciacchi, F. T., Rajendran, S. and Badwal, S. P. S. *J. Mater. Chem.*, 1997, **7**, 79.